



Research & Reviews In Electrochemistry

Full Paper

RREC, 6(2), 2015 [027-034]

Influence of the microstructure on the corrosion behaviour in a sulphuric solution of cast carbon steels as characterized by electrochemical impedance spectroscopy. Part 1: Effect of the carbon content

Manale Belhabib¹, Patrice Berthod^{1,2*}

¹Faculty of Sciences and Technologies, University of Lorraine, B.P. 70239, 54506 Vandoeuvre-lès-Nancy, (FRANCE)

²Institut Jean Lamour (UMR CNRS 7198), University of Lorraine, B.P. 70239, 54506 Vandoeuvre-lès-Nancy, (FRANCE)

E-mail: Patrice.Berthod@univ-lorraine.fr

ABSTRACT

The behaviour of carbon steels may depend on their microstructure, notably of their fraction in cementite which is piloted by the carbon content and of a previously underwent hardening. The case of the mechanical properties is well-known but the influences of the carbon content/cementite fraction and of an earlier plastic deformation on the corrosion behaviour is not necessarily so well determined. In this first part this is the carbon content which is under focus. A series of four binary Fe-C alloys, with C contents spread over the eutectoid composition, were elaborated following strictly the same synthesis parameters to avoid any perturbation of other factors such as various microstructure finenesses or presence of minor elements. Their behaviour in a model sulphuric acid solution was specified by spectroscopy of electrochemical impedance. Several differences were observed between on one hand the ferritic steel and on the other hand the three cementite-containing steels, concerning the evolution of the Nyquist half circle, the transfert resistance and the double layer capacity. © 2015 Trade Science Inc. - INDIA

KEYWORDS

Cast carbon steels;
Carbon content;
Corrosion;
Sulphuric acid;
Electrochemical impedance spectroscopy.

INTRODUCTION

The alloys based on both iron and carbon are very important for industry due to their numerous applications^[1]. The most simple and less expensive of them are carbon steels and not alloyed cast irons. The latter ones, first liquid alloy coming resulting from the reduction of iron ore in blast furnaces, can

present extremely various varieties due to the extreme diversity of the microstructures^[2-5] resulting from:

- * the existence of two diagrams (the stable austenite – graphite one and the meta-stable austenite – cementite one),
- * the possibility to solidify and to undergo the (pre-eutectoid if any then the) eutectoid transforma-

Full Paper

- tion exclusively in the first diagram or exclusively in the second one,
- * the possibility to solidify (entirely or only partly) in one of this diagram and to undergo the (pre-eutectoid if any then the) eutectoid transformation in the other diagram (here too entirely or partly),
 - * the possibility to present a pre-eutectic solidification of austenitic dendrites (hypo-eutectic cast-iron) or of either graphite (stable diagram) or coarse acicular cementite (meta-stable diagram),
 - * the possible shapes of graphite of cast iron solidified in the first diagram, this depending to an eventual more or less treatment of liquid iron (desulphuration, spheroidization, re-introduction of elements poisoning the spheroidal graphite growth),
 - * the heat-treatment of graphitization, ferritization, pearlite globularization,
 - * more or less fast and complex quenching,
 - * and so on...

Since they necessarily undergo solid state transformation in the meta-stable diagram since no graphite can precipitate at solidification in their cases, the carbon steels are more simple: ferritic (no carbon or extremely low C content), ferrite-pearlitic ($0 < \text{wt.}\% \text{ C} < 0.8$), pearlitic ($0.8 \text{ wt.}\% \text{ C}$), hyper-eutectoid ($0.8 < \text{wt.}\% \text{ C} < 2$) in case of not to fast cooling from the austenitic temperature domain down to room temperature. As for cast iron, more rapid cooling from the austenitic state allows obtaining not stable phases as bainite or martensite, or complex structures mixing ferrite, pearlite, bainite, martensite, if complex thermal evolutions chosen from the Time Temperature Transformation or Continuous Cooling Transformation are applied.

The microstructures (nature but also fineness) of carbon steels is well known to be of huge importance for their mechanical properties^[1-5], but it is possible that their surface reactivity can be also different following the microstructure, even if their chemical compositions are free of nickel, chromium...

In this work, the surface reactivity which was taken into consideration is the corrosion by an acidic aqueous solution, and the steels support of these in-

vestigation cast binary Fe-C alloys with C ranging from 0 to 1.6 wt.%. The microstructure parameter of interest was simply the amount in cementite, driven by the choice of the carbon content, for a given microstructure fineness fixed by the respect of a same thermal protocol for the elaboration of all alloys (same mass, same heating-isothermal stage-cooling laws, same ingot shape).

Among the numerous techniques usable for specifying the behaviour of corrosion this was here the association of a three-electrode cell and electrochemical impedance spectroscopy (EIS) which was chosen, since it allows both stationary and not stationary characterization of corrosion.

EXPERIMENTAL

Elaboration and as-cast microstructures of the alloys

Four carbon steels (Fe-xC alloys with $x=0, 0.4, 0.8$ and $1.6 \text{ wt.}\%$) were synthesized from pure elements by foundry. This was done in the water-cooled copper crucible of a high frequency induction furnace (CELES, France) with as operating parameters (Fe: Alfa Aesar > 99.9 wt.%, C: pure graphite): heating by progressive increase in injected power to 2500V, stage during about thirty seconds for a first thermal homogenization of the still solid parts of pure element, new increase in power up to 4000V leading to complete melting, three minutes stage for insuring total chemical homogenization of the liquid, then progressive cooling leading to solidification and solid state cooling. The obtained ingots, weighing 4 kg and displaying a compact shape, were cut to obtain several parts per steel.

One of them was destined for metallography investigations. It was embedded in a cold resin mixture (resin and hardener from ESCIL, France), then ground with SiC papers from 120-grit upto 2400-grit and polished with $1 \mu\text{m}$ hard particles until obtaining a mirror-like surface. After etched with Nital4 {ethanol-4% HNO_3 } it was observed by optical microscopy (Olympus BX51 equipped with a Toupcam digital camera driven by the Toupcam software).

Electrochemical measurements

Per alloy, a second part cut in the ingot was immersed in a liquid cold resin mixture by keeping a not covered upper part. After total stiffening they were extracted from the plastic mould, to be partly sewed in order to insert the denuded part of an electrical wire. Now in electrical contact the semi-embedded metallic parts were incorporated again in the mould. Additional liquid cold resin mixture was then poured, this time to immerse the upper part of the sample and the denuded copper. They were thus totally isolated from exterior, then from the electrolyte in which the electrode will be immersed. The emerging metallic part of the obtained electrode (working surface) was finally ground with papers from 120-grit to 1200-grit, washed and dried. The Counter Electrode (or auxiliary electrode) was a platinum one, and the electrode of potential reference was a Saturated Calomel one.

The electrochemical tests were carried out in a H_2SO_4 1M solution, using an Ametekpotentiostat driven by the Versastudio software. The tests consisted in measuring the free potential (E_{ocp}), then in applying to the working electrode a sinusoidal variation of potential (Eq. 1). The amplitude of variation was 10mV around E_{ocp} and the frequency varied from 100kHz down to 1 Hz. The resulting sinusoidal current (Eq. 2) was measured for five values of frequency by decade. The Nyquist $\{-Z_{im}$ versus $Z_{real}\}$ diagram was then plotted. This was repeated six times every ten minutes.

Since the half circle may be not complete or passed under the x-axis, the minimal value of Z_{real} was taken as being a good estimation of the electrolyte resistance Re and the maximal value of Z_{real} was taken as equal to $\{Re + Rt\}$, with consequently the determination of the transfert resistance Rt ^[6].

$$E = E_{ocp} + \Delta E \times \cos(\omega t) \quad (1)$$

$$I = I_0 \times \cos(\omega t + \phi) \quad (2)$$

Knowing that the summit of the half circle is obtained for the relation presented in (Eq. 3) the values of the corresponding frequency $f(-Z_{im} \text{ max})$ was noted, converted into pulsation $\omega(-Z_{im} \text{ max})$ according to equation (Eq. 4) which allows deducing the value of the double layer capacity C_{dc} by Eq. 5.

$$Rt \times C_{dc} \times \omega = 1 \quad (3)$$

$$\omega(-Z_{im} \text{ max}) = 2 \pi f(-Z_{im} \text{ max}) \quad (4)$$

$$C_{dc} = 1 / (Rt \times C_{dc}) \quad (5)$$

RESULTS AND DISCUSSION

Microstructures of the obtained alloys

After about ten seconds of immersion in the Nital solution the microstructure of the Fe-0.0C steel appears wholly ferritic (Figure 1). The Fe-0.4C steel is ferrite-pearlitic, the Fe-0.8C steel pearlitic and the Fe-1.6C steel hypereutectoid. The acicular shape of the pre-eutectoid ferrite (Fe-0.4C) as well as the one of the pre-eutectoid cementite (Fe-1.6C), thus of the Widmanstätten type, may be due to a too fast cooling (since, no longer maintained by magnetostriction, the ingot had entered in contact with the water-cooled copper crucible of the furnace).

Nyquist diagram versus time

The plot of the point $\{-Z_{im}(\omega)$ versus $Z_{real}(\omega)\}$ for the six successive times over one hour ($t=0$ min, 10 min, 20 min, 30 min, 40 min, 50 min and 60 min) is shown in Figure 2 for the Fe-0.0C steel, in Figure 3 for the Fe-0.4C steel, in Figure 4 for the Fe-0.8C steel and in Figure 5 for the Fe-1.6C steel.

The first fact that must be noted is that the half

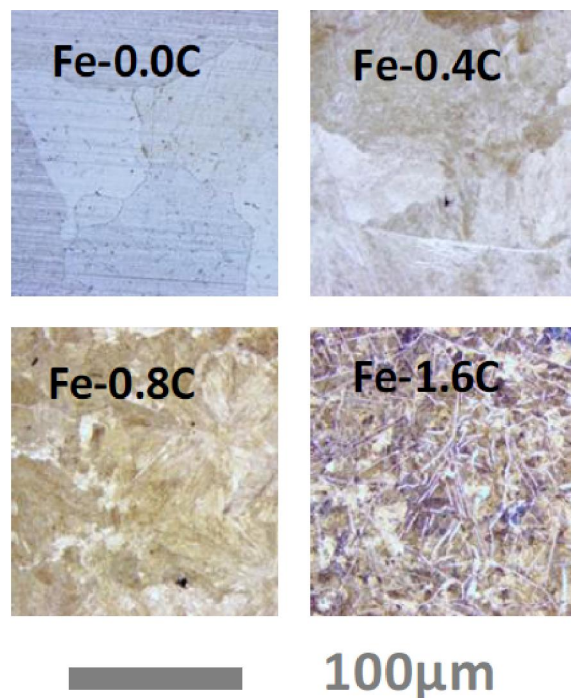


Figure 1 : Optical micrographs of the four steels after nital etching

Full Paper

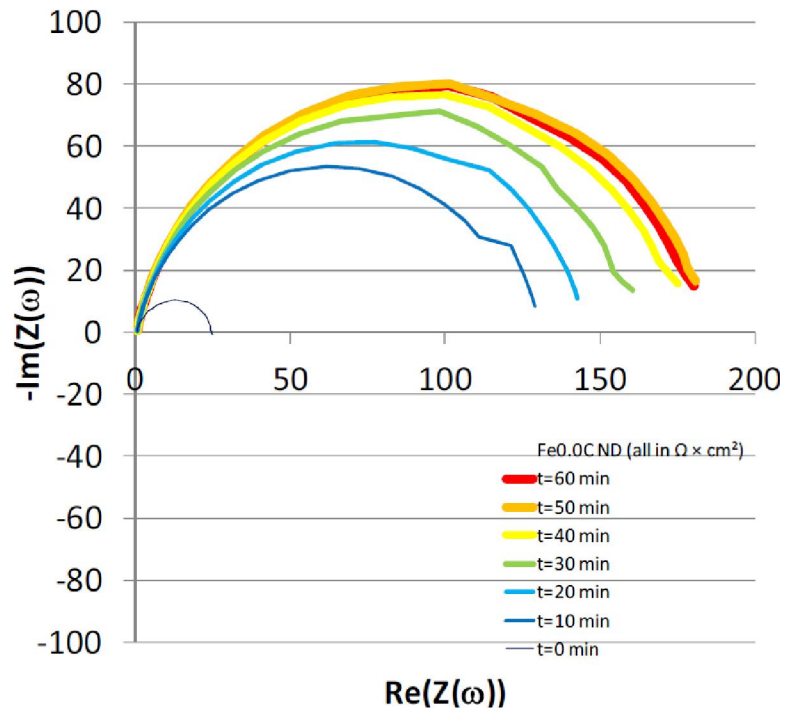


Figure 2 : Nyquist plot of the measured EIS values in the case of the Fe-0.0C steel

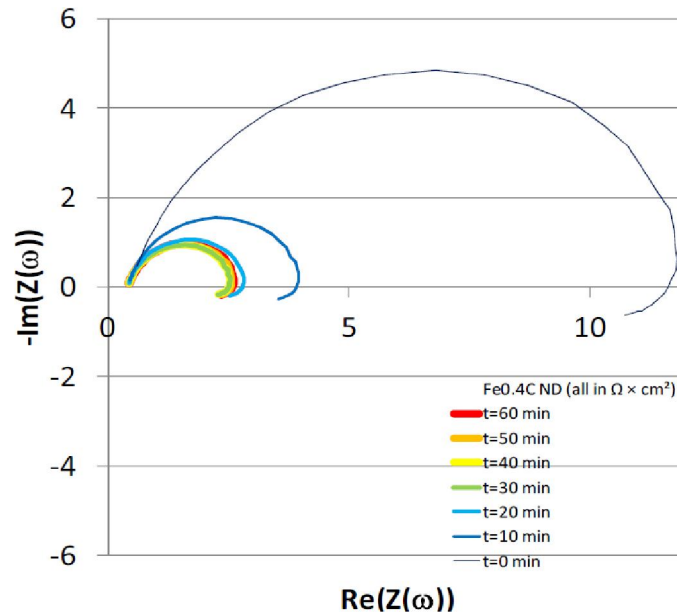


Figure 3 : Nyquist plot of the measured EIS values in the case of the Fe-0.4C steel

circle becomes greater and greater with time for the ferritic Fe-0.0C alloy while this is exactly the opposite phenomenon which occurs for the three other alloys. The second fact is that the curves are a little smaller than half a circle for the ferritic steel ($-Z_{im}$ already strictly positive for 1Hz) while it is in contrast a little greater for the three other alloys ($-Z_{im}$ strictly negative for 1Hz).

Since the electrolyte seems remaining constant

with time, this is the transfer resistance which seems increasing with time for the ferritic steel while it decreases with time for the three other steels. In all cases, whatever the evolution direction, the change of the semi-circle is fast during the beginning of immersion and thereafter it stabilizes.

Evolution of Re , R_t and C_{dc} versus time for the four alloys

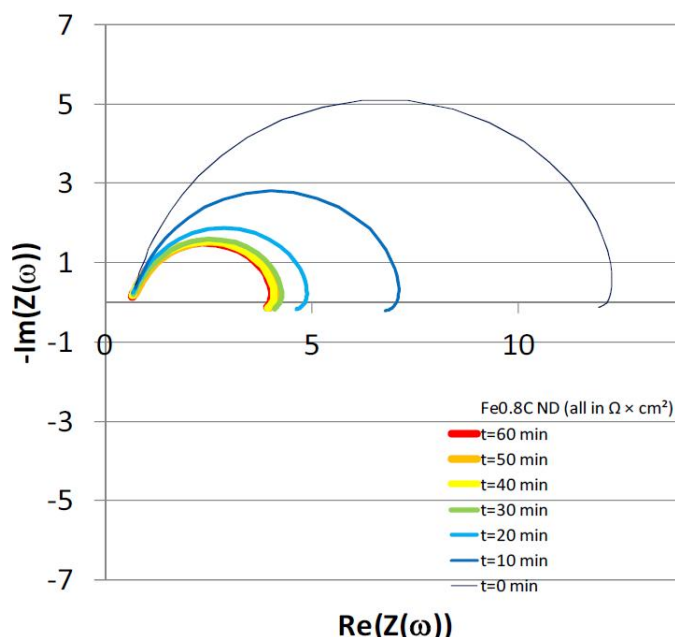


Figure 4 : Nyquist plot of the measured EIS values in the case of the Fe-0.8C steel

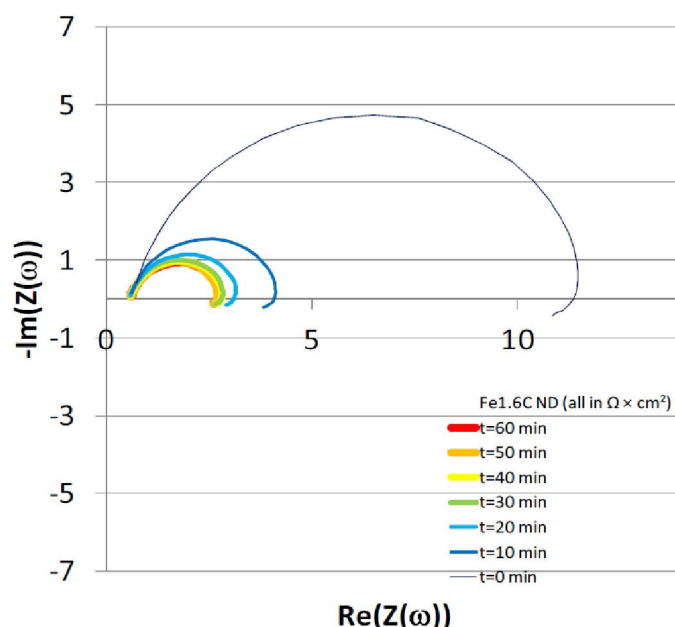


Figure 5 : Nyquist plot of the measured EIS values in the case of the Fe-1.6C steel

The electrolyte resistance does not vary significantly with time for each of the four alloys (Figure 6). There are small differences between the alloys but this is only due to a not real repeatability position of the working electrode by regards to the counter electrode. This is with no consequences for the more important results which follow.

The transfert resistance (Figure 7) is globally the same for the three cementite-containing steels ($C > 0$ wt.%), and its values decreases to stabilize, in all these three cases. The one of the ferritic steel

increases rapidly with time to stabilize at almost $180 \Omega \times \text{cm}^2$ (against about $3 \Omega \times \text{cm}^2$ for the three others) which suggests its passivation.

The double layer capacity remains globally constant versus time (about 8×10^{-5} Farad) for the ferritic steel while it increases to stabilize after 30-50 minutes for the three other steels. The higher stabilized value, almost ten times the ferritic steel one, was obtained for the hyper-eutectoid steel (1.6C): 60×10^{-5} Farad.

Full Paper

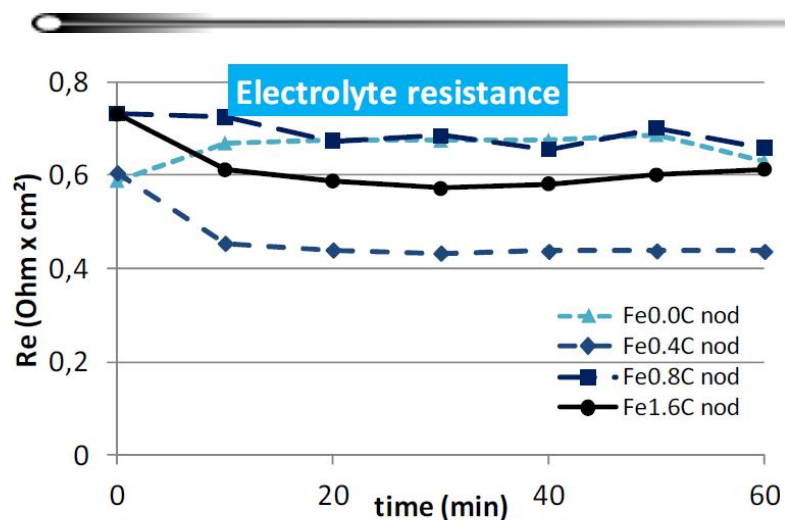


Figure 6 : Cumulated curves showing the evolution of the electrolyte resistance versus time during the 1 hour – immersion for the four steels

General commentaries

The first noticeable result which was obtained here is the superiority of the ferritic steel (Fe-0.0C) by comparison with the three binary steels. Its Nyquist semi-circle becomes greater and greater with time while the other steels know the opposite evolution. The transfert resistance, already higher than the ones of the others at $t = 0$ min, increases rapidly (and thereafter slower) while the transfert resistances of the other alloys tend decreasing, in contrast. The obtained values suggest that, initially in the active state, the ferritic alloy get passive, while the other steels remain in their active state at the same time. It is rather curious to see polycrystalline pure iron passivating in a solution the pH of which is almost zero. This is absolutely not predicted by the iron Pourbaix diagram^[7]. The principal difference between this ferritic alloy and usual ferritic steels – the fast cooling and $\gamma \rightarrow \alpha$ – is may be at the origin of this incoherence: to more deeply investigate this hypothesis one can think elaborating a series of carbon-free steels using the same Fe element as here, applying various cooling rate during solidification and the allotropic transformation, and testing them in corrosion using the same electrolyte, method and apparatus as here.

The second observation to point out concerns the double layer capacity: it is constant and rather low for the ferritic alloy while the ones of the three other steels vary, more precisely significantly increase. One can wonder that, since these three other

steels remain in an active state, as demonstrated by the low measured transfert resistances, either cementite (eutectoid for the Fe-0.4C and Fe-0.8C steels, and pre-eutectoid and eutectoid for the Fe-1.6C steel), or ferrite (pre-eutectoid and eutectoid for the Fe-0.4C steel, eutectoid for the Fe-0.8C and Fe-1.6C steels), is corroded faster than the other phase, with as result either an increase in electrolyte-ferrite or in electrolyte-cementite interfacial surface, with consequently an increase in double-layer capacity. Even if this not so clear (e.g. order between the $C_{dc} = f(t)$ curve of the Fe-0.4C steel and the one of the Fe-0.8C steel different than the one between the ferric steel and the hyper-eutectoid one), one can think that the low initial value ($t=0$) of the double layer capacity is to be attributed to ferrite since it is the principal phase present in all the tested steels, including the hyper-eutectoid one (equivalence of volume mass between ferrite and cementite + four times more ferrite than cementite in mass fraction in the Fe-1.6C steel). But when corrosion progresses, the ferrite which is a metal is probably more corroded than cementite which is a carbide, and the surface of contact between the acidic electrolyte and cementite increases while the one between the electrolyte and ferrite remains globally constant. So, the first interface, electrolyte-cementite, participates more and more at the total double layer capacity, which may explain the increase in time of the latter for the cementite-containing steels, which is additionally faster if cementite is more present (Fe-1.6C steel).

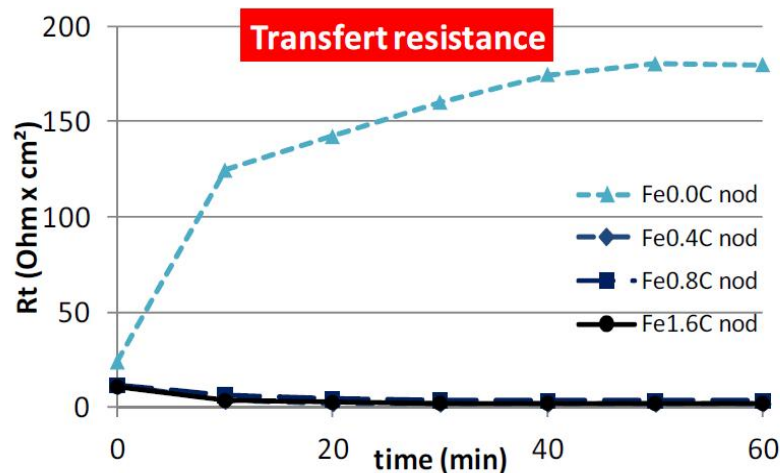


Figure 7a : Cumulated curves showing the evolution of the transfert resistance versus time during the I hour – immersion for the four steels

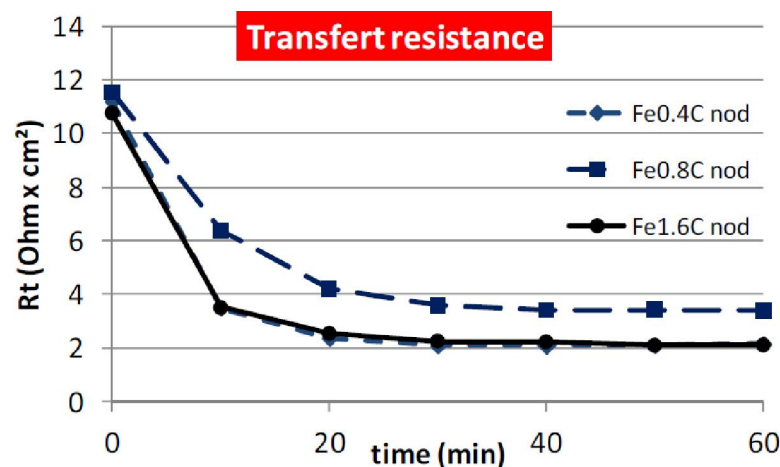


Figure 7b : Cumulated curves showing the evolution of the transfert resistance versus time during the I hour – immersion for the four steels (y-axis enlarged view of Figure 7a for the lowest Rt)

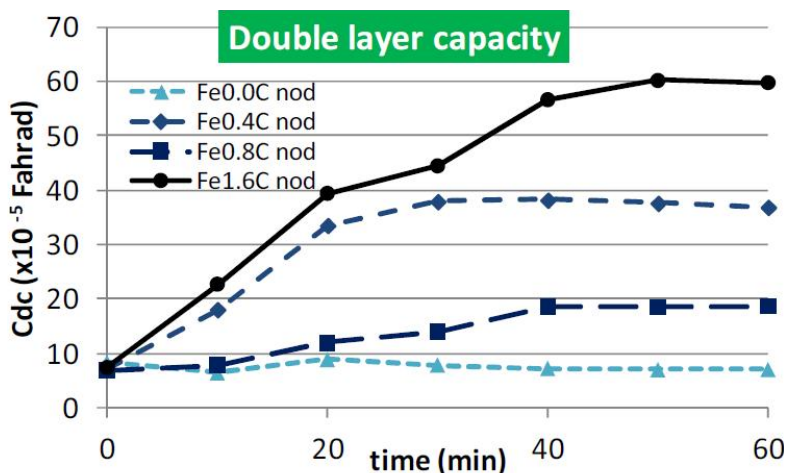


Figure 8 : Cumulated curves showing the evolution of the double layer capacity versus time during the I hour – immersion for the four steels

Elaborating a white cast-iron with the Fe-6.67wt.%C composition, e.g. only made of cementite (Fe_3C), and testing it as here done for the four steels, may allow verifying this hypothesis.

CONCLUSIONS

Even if some curious phenomena need to be verified then explained (ferritic steel passivating in H_2SO_4) some interesting results were obtained, notably on the differences (R_t , C_{dc}) between the ferritic steel and the hypo-eutectoid, eutectoid and hyper-eutectoid steels. In the second part of this work^[8] other parts cut from the same ingots will be plastically deformed and mounted as electrodes to carry out again EIS measurements. The aim will be to study if a hardening may influence the behaviours of these steels and how.

ACKNOWLEDGMENTS

The authors thank Mathieu Lierre for the preparation of the solution as well as for its assistance.

REFERENCES

- [1] J.M.Dorlot, J.P.Bailon, J.Masounave; "Des Matériaux", Editions de l'Ecole Polytechnique de Montréal, Montréal, (1986).
- [2] G.Béranger; Le livre de l'acier, Lavoisier, Paris Cachan, (1994).
- [3] J.R.Davis; Cast Irons, ASM International, (1996).
- [4] M.Durand-Charre; La Microstructure des aciers et des fontes. Genèse et interprétation, SIRPE, Paris, (2003).
- [5] M.Durand-Charre; Microstructure of steels and cast irons – engineering materials and processes, Springer-Verlag, Berlin Heidelberg New York, (2004).
- [6] C.Rochaix, Electrochimie, thermodynamique-cinétique, Nathan, Paris, (1996).
- [7] M.J.Pourbaix; Atlas of electrochemical equilibria in aqueous solution, Pergamon Press, Oxford, (1966).
- [8] M.Belhabib, P.Berthod; Research & Reviews in Electrochemistry, to be submitted.